

Modeling pulsed laser micromachining of micro geometries using machine-learning techniques

D. Teixidor · M. Grzenda · A. Bustillo · J. Ciurana

Received: 9 June 2013 / Accepted: 10 September 2013 / Published online: 26 September 2013
© Springer Science+Business Media New York 2013

Abstract A wide range of opportunities are emerging in the micro-system technology sector for laser micro-machining systems, because they are capable of processing various types of materials with micro-scale precision. However, few process datasets and machine-learning techniques are optimized for this industrial task. This study describes the process parameters of micro-laser milling and their influence on the final features of the microshapes that are produced. It also identifies the most accurate machine-learning technique for the modelization of this multivariable process. It examines the capabilities of laser micro-machining by performing experiments on hardened steel with a pulsed Nd:YAG laser. Arrays of micro-channels were manufactured using various scanning speeds, pulse intensities and pulse frequencies. The results are presented in terms of the main industrial requirements for any manufactured good: dimensional accuracy (in our case, depth and width of the channels), surface roughness and material removal rate (which is a measure of the productivity of the process). Different machine-learning techniques were then tested on the datasets to build highly accurate models for each output variable. The selected techniques were: k-Nearest Neighbours, neural networks, decision trees and linear regression models. Our analysis of the correlation coefficients and the mean absolute error of all the generated mod-

els show that neural networks are better at modelling channel depth and that decision trees are better at modelling material removal rate; both techniques were similar for width and surface roughness. In general, these two techniques show better accuracy than the other two models. The work concludes that decision trees should be used, if information on input parameter relations is sought, while neural networks are suitable when the dimensional accuracy of the workpiece is the main industrial requirement. Extensive datasets are necessary for this industrial task, to provide reliable AI models due to the high rates of noise, especially for some outputs such as roughness.

Keywords Machine learning-techniques · Laser process · Process parameters

Introduction

Laser systems are increasingly employed in many diverse micro-system technology sectors such as biomedicine, automotive manufacture, telecommunications, display devices, printing technologies and semiconductors (Rizvi and Apte 2002). Material removal during the laser-machining process depends, to a certain degree, on the characteristics of the laser and the properties of the workpiece; however, it is primarily determined by the interaction between the laser and the workpiece (Pham et al. 2007). In real factory conditions, this interaction is influenced by other types of machine-tool parameters that are easily controlled, such as pulse frequency, peak power, scanning speed and overlapping. Although many of these process parameters can be adjusted, in order to obtain the desired quality and to optimize the efficiency of the features being produced, there is a lack of knowledge about how they affect the laser machining process, especially in

J. Ciurana (✉) · D. Teixidor
Department of Mechanical Engineering and Industrial
Construction, Universitat de Girona, Girona, Spain
e-mail: quim.ciurana@udg.edu

M. Grzenda
Faculty of Mathematics and Information Science, Warsaw
University of Technology, Warsaw, Poland

A. Bustillo
Department of Civil Engineering, University of Burgos,
Burgos, Spain

new sensitive applications such as micro-machining of the shape of micro geometries (Brousseau and Eldukhri 2011).

Various studies have investigated how laser process parameters affect the quality of the resultant machined features. Campanelli et al. (2007) analyzed the influence of frequency, scanning strategy and overlap on depth and surface roughness, during laser machining of an aluminum-magnesium alloy. Various experiments and variance analysis have demonstrated that, in general, optimizing surface roughness is conversely related to depth maximization. Cicală et al. (2008) studied the effects of pulse frequency, power, scanning speed and overlap on the MRR and surface roughness. The results showed that pulse frequency and scanning speed were the main parameters affecting surface roughness, which was reduced with lower scanning speeds and higher frequencies. The Material Removal Rate (MRR) mainly depends on pulse frequency alone. Bartolo et al. (2006) analyzed the incidence of the same parameters while looking at the scanning strategy, in the machining of channels in tempered steel and aluminum. Their results suggested that surface quality is better at lower frequencies and reduced laser power. However, both parameters need to be increased, in order to achieve an optimum value for a higher MRR. Kaldos et al. (2004) used a CNC milling machine with a Nd:YAG laser source, on die steel, to study the impact of lamp current, pulse frequency, overlapping and scanning speed on surface roughness and the MRR. They concluded that an increase in current intensity or insufficient overlap of laser passes results in a less well finished surface. Semaltianos et al. (2010) studied the effects of fluence and pulse frequency on surface roughness and MRR in nickel-based alloys with a Nd:YVO₄ picosecond laser. They also analyzed the surface morphology of these alloys with AFM and SEM techniques.

Ciurana et al. (2009) used a pulsed Nd:YAG laser to study the effect of the process parameters on minimum volume error and surface roughness in laser machined tool steel for macro scale geometry, although micro scale geometry was not evaluated. The experimental results were inconsistent for large shapes. Dhara et al. (2008) micro-machined die steel while modifying pulse intensity, pulse frequency, pulse duration and air pressure, in order to predict the optimum process parameter settings for maximum depth with a minimum recast layer. Kumar and Gupta (2010) investigated the influence of laser power, pulse frequency, number of scans and air pressure, on the groove depth in the generation of micro-notches with a nanosecond pulsed fiber laser on stainless steel and aluminum. Karazi et al. (2009) machined and characterized micro-channel formation by laser machining. They studied the effects of laser power, pulse frequency and scanning speed on the width and depth of the channels. They also modeled the process using Artificial Neural Networks (ANN).

The application of Artificial Intelligence (AI) techniques to model the micro machining of metal components is an open

issue. Most of the very few works on this topic have focused on the application of ANNs to this task: the work of Desai and Shaikh (2012) predicted the depth of cut for single-pass laser micro-milling process using ANN and genetic programming approaches and the work of Karazi et al. (2009) compared ANN and DoE models for the prediction of laser-machined micro-channel dimensions. All these works refer only to geometrical dimensions and do not model other outputs of industrial interest, such as productivity and surface roughness. Other kinds of AI techniques, such as decision trees, Bayesian Networks, and ensembles have not been tested in this industrial context. If the state of the art can include the application of AI techniques to machining processes similar to laser milling, we can conclude that ANNs are the most common technique used for most of these processes such as milling, drilling or laser finishing (Quintana et al. 2011, 2012; Chandrasekaran et al. 2010), although many other AI techniques have also been applied for such purposes. Bustillo et al. proposed the use of Bayesian Networks and ensembles to predict surface roughness in drilling (Bustillo and Correa 2012), laser finishing (Bustillo et al. 2011a) and roughing (Bustillo et al. 2011b) operations, Grzenda et al. (2012a, b) proposed different evolutionary algorithms to improve ANN accuracy in drilling and milling operations, and Mahdavinjad et al. (2012) proposed the use of artificial immune systems to model milling processes. In any case, most of the most recent works, such as those proposed by Bustillo et al. (2011b), Correa et al. (2009), Desai and Shaikh (2012), Mahdavinjad et al. (2012) and Díez-Pastor et al. (2012), all use ANNs as a standard technique to be improved by new approaches.

The aim of this work is to describe the information needed to improve the laser micro-machining process in the production of microshapes and to develop a suitable AI model for the modelization of this industrial task. The process parameter settings are studied with statistical tools and optimized with models developed from experimental work, to achieve the required dimensional precision, surface quality and productivity. The experimental section consists in fabricating arrays of micro-channels on hardened tool steel using laser machining processes, while measuring feature size, geometric accuracy, surface roughness and the MRR. This work will contribute to the selection of appropriate process parameters through an analysis of the influence of scanning speed, pulse frequency and pulse intensity on the final quality of the machined micro-feature. Moreover, machine-learning methods are used to evaluate the complexity of prediction tasks. Representatives of rule-based, instance-based, and both linear and nonlinear models are applied. Prediction accuracy remains at different levels depending on the parameter to be modeled rather than the technique used to model it. Hence, the complexity of modeling individual features of particular interest may be more easily determined.

Experimental set up

The experiments, set up to study the influence of the process parameters, were performed with a pulsed Nd:YAG, Deckel Maho Lasertec 40 machine, with 100 W average laser power and a wavelength of 1,064 nm.

Although the pulse intensity level on the surface was not measured during our experiments, based on the technical data of the laser system, we can provide an ideal pulse intensity level, which is given by:

$$PI = \frac{P}{\pi \left(\frac{d}{2}\right)^2} \quad (1)$$

where, P is the laser power (100 W), and d is the beam spot diameter (0.003 cm). Therefore the ideal pulse intensity was estimated to be 1.4 W/cm². Furthermore, we can determine the ideal Peak Pulse Power (PPP), which is given by:

$$PPP = \frac{P}{\tau} \quad (2)$$

where, P is the laser power (100 W) and τ is the laser pulse duration (10 ns). For the laser characteristics used in this study, the PPP is estimated to be 10 MW/s. The specifications of the micro channels are: 200 μ m in width (W) and 50 μ m in depth (D), machined by the motion of the laser beam in the x and y directions removing material in all three directions (x , y and z). As shown in Fig. 1, in order to machine the entire cavity, there is overlap between adjacent pulses (O_y) within a pass of length (L) and overlap between successive passes (O_x). All the experiments were performed with a

laser spot size (\varnothing) of 0.03 mm and a track displacement (distance between passes, a) of 10 μ m. The overlap O_x between successive passes is given by (Samant and Dahotre 2010):

$$O_x = \left(1 - \frac{a}{\varnothing}\right) \times 100 \quad (3)$$

In this study, O_x was 66.6 %. The overlap between adjacent pulses (O_y) depends on the scanning speed, the pulse frequency and the spot diameter. It is therefore different for each experiment. O_y is given by:

$$O_y = \left(1 - \frac{SS}{PF \times \varnothing}\right) \times 100 \quad (4)$$

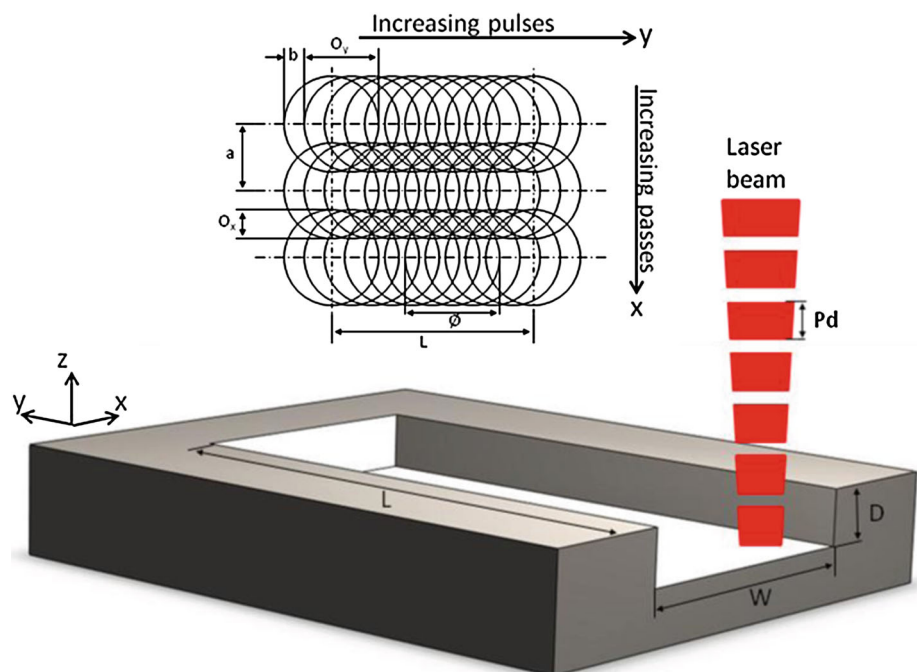
where, SS is the scanning speed and PF is the pulse frequency, which are different for each experiment.

Hardened AISI H13 tool steel was selected as the work-piece material, because it is widely used in the moulds and dies industry.

Dimensional measurements were performed with a ZEISS SteREO Discovery.V12 stereomicroscope. Quartz PCI© software was used to measure the feature dimensions and Mitutoyo SV2000 Surftest equipment was used to measure surface roughness.

Some screening experiments were performed to select the appropriate factor levels of the process parameters. **Several micro-channels were machined, in each case changing one single parameter while the others remained fixed. In this way, we could observe the impact of each single control variable, in order to determine the control parameter range.** This pre-

Fig. 1 A schematic illustration of the 3D-laser milling process and overlapping laser pulses



evaluation provides a full factorial design with the variable factors and factor levels presented in Table 1, which is then used to study the influence of the input parameters on the finished workpiece, for which the response parameters are surface roughness (μm), the MRR (mm^3/min) and the width and depth dimensions (μm). Similar experimental studies have been conducted in earlier works. Statistical analyses have pointed out that pulse frequency is the least relevant of the three factors that were studied. Thus, just two levels for these parameters were selected, while nine levels were established for the scanning speed, in order to conduct an in-depth study of its effect on the responses.

Experimental results and discussion

Following the design of the experiments summarized in Table 1, 54 micro channels were machined with the laser machining process. Surface roughness was measured in five different sections of each micro-channel to get the mean value of the entire channel. Then, each channel was cut into three parts to get the cross-section profiles, from which the measurements of depth and width were taken by processed digital images. Once again, five different measurements, proportionally distributed along the depth and the width, were measured. The area removed was also measured for each channel profile, in order to calculate the MMR. The mean values of the experimental results obtained from the machined features for all the combinations of the variable factors are shown in Table 2.

The micro-channels presented variations in dimensions and shape. These variations are clearly represented in Fig. 2, which presents the images of six micro-channels. Analysis of Variance was performed for each response factor, to study the influence of the process parameters.

Micro-channel depth

As can be seen in Table 2, which shows the results obtained for the micro-channel depths, the target depth of $50\text{ }\mu\text{m}$ was never reached. This is clear in Fig. 3, where the influence of the scanning speed and the pulse intensity on the depth dimension is summarized. It shows that almost all of the

machined depths are within the $10\text{--}25\text{ }\mu\text{m}$ range and only few experiments achieved depth values above this range.

The trend lines presented in Fig. 3 clearly show that higher scanning speeds result in smaller depths and higher pulse intensities result in deeper micro-channels. Thus, the greatest depth was reached with the lowest scanning speed (200 mm/s) and the highest pulse intensity (45%). In a laser-milling process (with 3D movements), slower displacements of the laser beam means that the surface is machined with high energy for a longer time, which allows a larger amount of energy to be absorbed by the material resulting in channels of greater depths. This demonstrates that higher pulse intensity values would be necessary to obtain depth values closer to the target.

Table 3 summarizes the ANOVA results, revealing that the most significant factors for the average depth of micro-channels were scanning speed and pulse intensity, as previously pointed out ($p < 0.005$). The F-values indicate that pulse intensity was the most significant factor, which is made clearer by the contribution values.

Compared with other authors, the experimental results shows that higher pulse intensity and lower scanning speeds tend to give deeper channels, which is in line with the idea that the number of pulses per mm increases, as the laser beam moves more slowly across the workpiece, thus removing more material. Furthermore, when the intensity is higher, the pulse energy increases, which in turn results in greater depth values (Bordatchev and Nikumb 2003; Yousef et al. 2003).

Micro-channel width

Table 2 presents width dimensions that range from 175.5 to $197.7\text{ }\mu\text{m}$. Once again, no experiment achieved the target value ($200\text{ }\mu\text{m}$). Figure 4 shows how the scanning speed and the pulse intensity affected the average width. In this case, in contrast to the results on depth, the experimental values were closer to the target width when the scanning speed was high and the pulse intensity was low. These converse effects on width and depth are due to the fact that straight walls are really difficult to achieve. Thus, as the channel becomes deeper, the width becomes narrower, producing a smaller mean width value.

Table 4 summarizes the results of the ANOVA analysis on the average width. It can be seen that the pulse frequency has no statistically significant effect on width dimension. The parameters that do have a significant effect on the width are pulse intensity and scanning speed, with pulse intensity being the most significant, as is clearly indicated by the results of the F-value, with a contribution of 69.5% .

Although other studies using single laser shots (Bordatchev and Nikumb 2003; Yousef et al. 2003) have concluded that crater depth and diameter increase with pulse

Table 1 Variable factors and factor levels

| Variable factors | Factor levels | | |
|----------------------------|---------------|-----|-----|
| Scanning speed (SS) (mm/s) | 200 | 225 | 250 |
| | 275 | 300 | 325 |
| | 350 | 375 | 400 |
| | 35 | 40 | 45 |
| Pulse intensity (PI) (%) | 35 | 40 | 45 |
| Pulse frequency (PF) (kHz) | 35 | 40 | – |

Table 2 DoE with the experimental results

| # | PI (%) | PF (kHz) | SS (mm/s) | depth (μm) | width (μm) | Ra (μm) | MRR (mm ³ /min) | # | PI (%) | PF (kHz) | SS (mm/s) | depth (μm) | width (μm) | Ra (μm) | MRR (mm ³ /min) |
|----|--------|----------|-----------|------------|------------|---------|----------------------------|----|--------|----------|-----------|------------|------------|---------|----------------------------|
| 1 | 35 | 35 | 200 | 18.3 | 189 | 0.505 | 0.034 | 28 | 35 | 40 | 200 | 13.9 | 192.9 | 0.560 | 0.025 |
| 2 | 35 | 35 | 225 | 17.4 | 190 | 0.477 | 0.036 | 29 | 35 | 40 | 225 | 12.6 | 175.5 | 0.479 | 0.017 |
| 3 | 35 | 35 | 250 | 14.9 | 191 | 0.533 | 0.034 | 30 | 35 | 40 | 250 | 11.6 | 188.1 | 0.531 | 0.026 |
| 4 | 35 | 35 | 275 | 15.7 | 195.8 | 0.455 | 0.041 | 31 | 35 | 40 | 275 | 15.7 | 191.6 | 0.465 | 0.034 |
| 5 | 35 | 35 | 300 | 12.9 | 197.7 | 0.456 | 0.033 | 32 | 35 | 40 | 300 | 8.1 | 193.2 | 0.506 | 0.026 |
| 6 | 35 | 35 | 325 | 11.6 | 193.2 | 0.463 | 0.027 | 33 | 35 | 40 | 325 | 8.1 | 189.8 | 0.520 | 0.020 |
| 7 | 35 | 35 | 350 | 8.1 | 191.7 | 0.470 | 0.019 | 34 | 35 | 40 | 350 | 11.6 | 189.2 | 0.471 | 0.034 |
| 8 | 35 | 35 | 375 | 10.9 | 192.5 | 0.504 | 0.021 | 35 | 35 | 40 | 375 | 10.8 | 189.9 | 0.525 | 0.027 |
| 9 | 35 | 35 | 400 | 10.2 | 192.8 | 0.457 | 0.027 | 36 | 35 | 40 | 400 | 11.7 | 190.1 | 0.463 | 0.027 |
| 10 | 40 | 35 | 200 | 29.9 | 183.9 | 0.549 | 0.055 | 37 | 40 | 40 | 200 | 31.2 | 186.1 | 0.531 | 0.065 |
| 11 | 40 | 35 | 225 | 30.0 | 184.9 | 0.481 | 0.059 | 38 | 40 | 40 | 225 | 26.2 | 186.6 | 0.571 | 0.061 |
| 12 | 40 | 35 | 250 | 25.4 | 184.4 | 0.513 | 0.061 | 39 | 40 | 40 | 250 | 23.7 | 187.3 | 0.462 | 0.056 |
| 13 | 40 | 35 | 275 | 21.9 | 187.2 | 0.664 | 0.048 | 40 | 40 | 40 | 275 | 17.1 | 190.4 | 0.510 | 0.026 |
| 14 | 40 | 35 | 300 | 16.8 | 189.9 | 0.478 | 0.036 | 41 | 40 | 40 | 300 | 17.7 | 195.7 | 0.459 | 0.041 |
| 15 | 40 | 35 | 325 | 14.4 | 188.4 | 0.473 | 0.032 | 42 | 40 | 40 | 325 | 19.2 | 192.3 | 0.461 | 0.061 |
| 16 | 40 | 35 | 350 | 18.5 | 188.5 | 0.485 | 0.041 | 43 | 40 | 40 | 350 | 17.3 | 190.3 | 0.435 | 0.039 |
| 17 | 40 | 35 | 375 | 18.2 | 190.5 | 0.457 | 0.048 | 44 | 40 | 40 | 375 | 16.5 | 190.5 | 0.490 | 0.044 |
| 18 | 40 | 35 | 400 | 18.4 | 190.0 | 0.382 | 0.043 | 45 | 40 | 40 | 400 | 14.2 | 192.3 | 0.423 | 0.040 |
| 19 | 45 | 35 | 200 | 39.6 | 184.4 | 0.519 | 0.065 | 46 | 45 | 40 | 200 | 38.6 | 184.4 | 0.519 | 0.074 |
| 20 | 45 | 35 | 225 | 35.8 | 184.1 | 0.513 | 0.073 | 47 | 45 | 40 | 225 | 35.0 | 184.2 | 0.531 | 0.067 |
| 21 | 45 | 35 | 250 | 33.7 | 181.0 | 0.493 | 0.072 | 48 | 45 | 40 | 250 | 29.5 | 180.7 | 0.526 | 0.071 |
| 22 | 45 | 35 | 275 | 22.1 | 184.3 | 0.443 | 0.063 | 49 | 45 | 40 | 275 | 26.8 | 185.3 | 0.523 | 0.056 |
| 23 | 45 | 35 | 300 | 25.4 | 186.2 | 0.451 | 0.057 | 50 | 45 | 40 | 300 | 25.1 | 187 | 0.514 | 0.067 |
| 24 | 45 | 35 | 325 | 26.5 | 189.2 | 0.451 | 0.061 | 51 | 45 | 40 | 325 | 22.8 | 186.8 | 0.446 | 0.062 |
| 25 | 45 | 35 | 350 | 20.8 | 191.1 | 0.447 | 0.047 | 52 | 45 | 40 | 350 | 19.3 | 187.3 | 0.509 | 0.039 |
| 26 | 45 | 35 | 375 | 19.8 | 189.9 | 0.397 | 0.054 | 53 | 45 | 40 | 375 | 17.5 | 187.6 | 0.408 | 0.040 |
| 27 | 45 | 35 | 400 | 19.1 | 188.3 | 0.377 | 0.049 | 54 | 45 | 40 | 400 | 17.7 | 188.6 | 0.413 | 0.040 |

energy, the width decreased in our case. This effect can be explained by the laser-milling process that needed several passes along all axes to obtain the final shape. Thus, because of the difficulty in achieving straight walls, due the Gaussian shape of the laser beam, the width of the channel narrowed as it became deeper. Therefore, the mean width of the channel decreased.

Micro-channel surface roughness

The influence of the variable factors on surface roughness was also evaluated. Figure 5 shows the effect of the scanning speed and the pulse intensity on surface roughness. The trend lines indicate that surface roughness decreased at high scanning speeds. The influence of pulse intensity is less clear, although it does appear to suggest that a higher intensity resulted in lower surface roughness. Slow scanning speeds did not improve surface roughness and fast

movements hardly affected it. Furthermore, the experimental results showed no large differences, with a range between 0.4 and 0.55 μm. The best surface roughness values were obtained with a combination of the highest pulse intensity and highest scanning speed.

Table 5 summarizes the results of the ANOVA, revealing that scanning speed was the most significant factor in surface roughness, while neither pulse intensity nor pulse frequency had a statistically significant effect on the same variable. However, the contribution of the scanning speed was relatively slight at 46.1 %.

Our experimental results showed that high pulse intensities and slower scanning speeds meant that more energy was applied to the workpiece, increasing the damage caused to the surface. Therefore, lower pulse intensities and higher scanning speeds will improve the final quality of the machined parts, because surface roughness will be reduced (Bordatchev and Nikumb 2003).

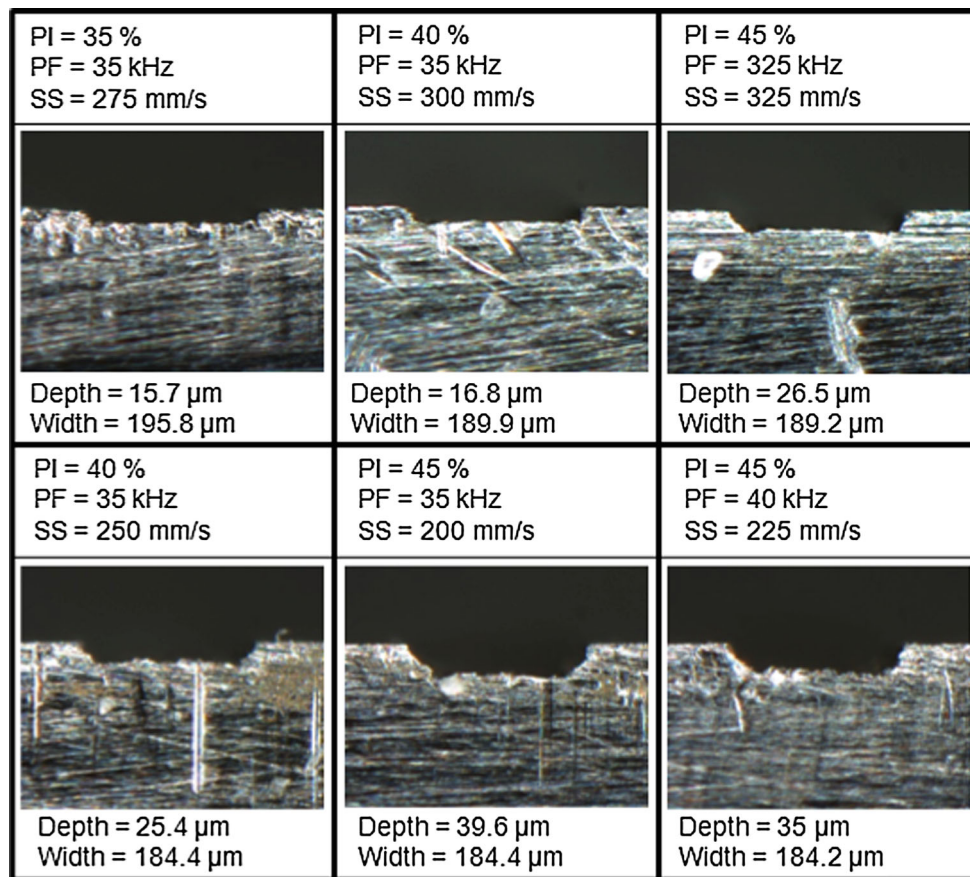


Fig. 2 Images of micro-channels

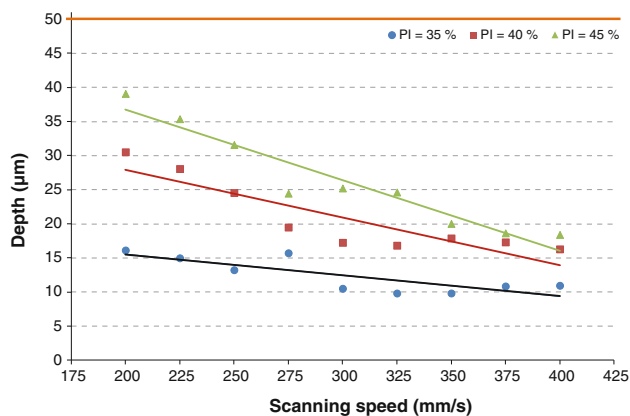


Fig. 3 Influence of scanning speed and pulse intensity on depth dimension

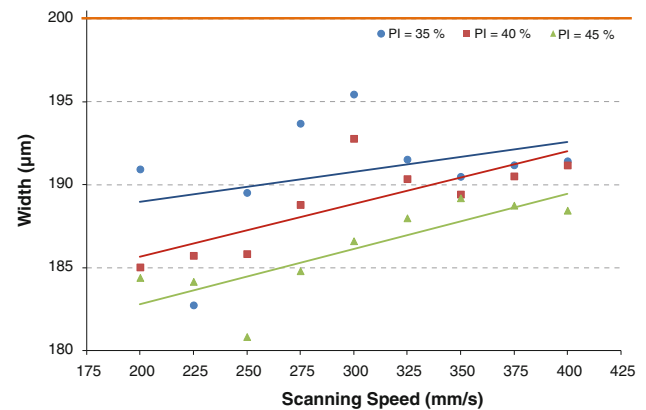


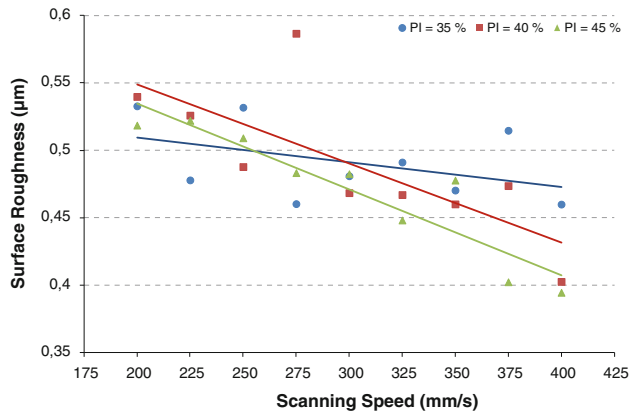
Fig. 4 Influence of scanning speed and pulse intensity on width dimension

Table 3 ANOVA analysis for depth

| Factor | Degrees of freedom (DOF) | Sum of squares (SS) | Mean squares (MS) | F-value | P value | Contribution (%) |
|--------|--------------------------|---------------------|-------------------|---------|---------|------------------|
| PI | 2 | 1775.26 | 887.63 | 94.72 | 0.000 | 83.9 |
| PF | 1 | 25.43 | 25.43 | 2.71 | 0.107 | 2.4 |
| SS | 8 | 1163.59 | 145.45 | 15.52 | 0.000 | 13.7 |

Table 4 ANOVA analysis for width

| Factor | Degrees of freedom (DF) | Sum of squares (SS) | Mean squares (MS) | F | P | Contribution (%) |
|----------|-------------------------|---------------------|-------------------|-------|-------|------------------|
| PI | 2 | 195.88 | 97.94 | 12.15 | 0.000 | 69.5 |
| PF | 1 | 5.01 | 5.01 | 0.62 | 0.435 | 3.5 |
| SS | 8 | 304.22 | 38.03 | 4.72 | 0.000 | 27 |
| Residual | 42 | 338.43 | 8.06 | – | – | – |

**Fig. 5** Influence of scanning speed and pulse intensity on surface roughness

Micro-channel material removal rate

The effect of the process parameters on the MRR was also studied. Figure 6 presents the effects of pulse intensity and scanning speed on the MRR. The trend lines clearly indicate that MRR increased at lower scanning speeds and higher pulse intensities. Although higher scanning speeds resulted in faster processes, the area of material removal was smaller, so the MRR decreased. On the other hand, a higher pulse intensity resulted in deeper channels and, in consequence, higher MRRs.

The ANOVA results for MRR are shown in Table 6. It can be seen that pulse frequency had no statistically significant effect on MRR. Pulse intensity was found to have the most significant effect on MMR with a contribution of 93.1 %, while scanning speed had a somewhat lesser impact, with a contribution of 5.9 %.

As MRR is directly proportional to the width and depth of the channel, the MRR plot has a shape that is similar to the depth plot, due to the fact that the influence of the depth is greater than that of the width.

Modeling

The ability of different models to predict features of interest

Following the experimental tests, the study and ANOVA analysis of the relationship between the parameters, various

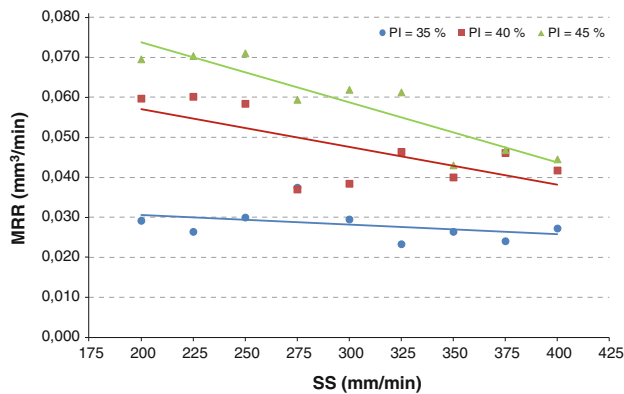
machine-learning techniques were then selected and tested for depth and width dimension, surface roughness and MRR, in order to determine their correlation with the process parameters. The objective was to obtain the most appropriate process parameters for producing minimal surface roughness with the highest material removal rate. This selection included the k-Nearest Neighbours (kNN) technique with k set to 1, ..., 5, linear regression, decision trees, and multilayer perceptrons. Hence, these methods were considered as they have clear decision rules and the capability to perform both linear and nonlinear transformations on the input data.

A 10-fold cross-validation was applied, which takes account of the capability of the models to predict output parameter values from new input data. More precisely, it was used to estimate the accuracy of a model built with a machine-learning technique that incorporated certain unique settings. First, the entire data set was first divided into 10 non-empty subsets. Then, each subset was used for testing the model, which was previously constructed with both the technique and its settings on the sum of the remaining subsets. This process was repeated 10 times. The correlation coefficients calculated from the testing subsets show whether the combination of the machine-learning technique and its settings can develop models that are capable of predicting the value of the parameter of interest such as depth. Importantly, this capability was tested for new inputs not used in the construction of the models. The correlation coefficients reported in this section were calculated in this way.

In addition, a single model built with the entire available data set was constructed for every output parameter and every technique. The correlation coefficient for the model that was built and tested with the same entire data set is reported in brackets for the multilayer perceptron, decision tree and linear regression in Tables 8, 9, 10, 11 and 12. A substantial difference can frequently be observed between the ability of the technique such as decision tree to model known cases and to predict the feature of interest for new process settings. This is most clearly seen for the 1 nearest neighbour classifier, which yielded the correlation of 1 on the data set with which it was constructed. It simply remembers each pattern with which it was developed and uses the pattern to give a direct response with the requested value of the parameter of

Table 5 ANOVA analysis for surface roughness

| Factor | Degrees of freedom (DF) | Sum of squares (SS) | Mean squares (MS) | F | P | Contribution (%) |
|----------|-------------------------|---------------------|-------------------|------|-------|------------------|
| PI | 2 | 0.004 | 0.002 | 1.92 | 0.160 | 13.4 |
| PF | 1 | 0.005 | 0.005 | 5.79 | 0.021 | 40.5 |
| SS | 8 | 0.051 | 0.006 | 6.58 | 0.000 | 46.1 |
| Residual | 42 | 0.039 | 0.001 | – | – | – |

**Fig. 6** Influence of scanning speed and pulse intensity on MRR

interest. Thus, no correlation coefficients for the training set were reported for NN classifiers.

The results of a sample machine-learning parameter selection are discussed in greater detail in “The selection of machine-learning parameters in the example of decision trees” section. As each technique is associated with its own set of parameters, decision trees were selected for more detailed analysis. The key parameters for the remaining models are: k value for kNN, the number of hidden neurons for multilayer perceptrons and the selection of attributes for linear regression.

A naïve approach was adopted as a baseline to analyse the prediction of the individual parameters listed above and to ensure that the new models extracted useful information from the dataset. The naïve approach is based on using the mean values of a parameter as a prediction of its parameter value. The prediction produced by the naïve method is always the same, irrespective of the values of the process parameters. As a consequence, the higher the difference between the correlation coefficient attained for the machine-learning model such as neural network and naïve method, the greater the ability of the machine-learning model to capture the impact of process parameters on the parameter of interest e.g. depth. Should the two correlation coefficients for the naïve method and machine-learning method remain at a similar level, the benefits of using the latter method would be questionable. More precisely, this would mean that the quality of predictions developed with the machine-learning method was similar to random guessing.

Hence, the correlation coefficient (R^2) and Mean Absolute Error (MAE) for individual input parameters modelled with the naïve approach were analysed first of all. The results are shown in Table 7, in which it may be seen that the correlation coefficients for the four models with the naïve approach are very low.

Starting with the low accuracy provided by a naïve approach, different machine-learning models were built for each output parameter. First, the accuracy, in terms of R^2 and MAE, of the depth modelling are shown in Table 8. The best results for the training set are observed for decision trees. However, multilayer perceptrons yielded the best accuracy for cross-validation (in bold in Table 8) and the highest correlation. It can be observed that 1NN is the best technique out of all the kNN simulations under analysis. This suggests limited noisiness of depth, i.e. the most similar input features provide the best estimation of the output parameter.

It is worth noting here that the accuracy of both the decision tree and the multilayer perceptron is quite similar, which suggests that the decision tree is better adapted to industrial applications. It also provides a clear explanation of the way the parameter of interest is estimated, which in this case is depth. It is interesting to investigate the definition of the tree shown in Fig. 7. As is clear from the ANOVA analysis, pulse intensity is the main parameter (83.9 %) for this process. The first node therefore refers to this parameter; scanning speed is the second parameter from the ANOVA analysis (13.7 %) and forms the second nodal level of the tree; leaving the last level for the parameter with the weakest influence: pulse frequency. It is also interesting to see how the tree generates the final leaves at different scanning speeds, depending on the pulse intensity; which was expected considering the relation between both parameters shown in Fig. 3. This capability of the decision tree, which produced clear graphical conclusions when modelling the influence of each parameter, makes them the most interesting technique. Moreover, **the linear regression models failed to achieve the required accuracy**, a result that fits in well with the conclusion presented in “Experimental results and discussion” section: that channel depth depends mainly on scanning speed and pulse intensity and that this dependency is not linear.

Next, the results for width were analysed. These results are shown in Table 9. The best method on the training set turned out to be a decision tree, which suggests that a nonlinear

Table 6 ANOVA analysis for MRR

| Factor | Degrees of freedom (DF) | Sum of squares (SS) | Mean squares (MS) | F | P | Contribution (%) |
|----------|-------------------------|-----------------------|-----------------------|-------|-------|------------------|
| PI | 2 | 0.0086 | 0.0043 | 57.92 | 0.000 | 93.1 |
| PF | 1 | 4.82×10^{-5} | 4.82×10^{-5} | 0.65 | 0.424 | 1 |
| SS | 8 | 0.0021 | 0.0002 | 3.65 | 0.003 | 5.9 |
| Residual | 42 | 0.0031 | 7.4×10^{-5} | – | – | – |

Table 7 Naïve prediction for individual parameters

| Parameter | Correlation coefficient (R^2) | Mean absolute error (MAE) |
|-----------------------------|-----------------------------------|---------------------------|
| Depth | 0.178 | 6.49 |
| Width | 0.133 | 3.078 |
| Surface roughness (R_a) | 0.239 | 0.0397 |
| MRR | 0.178 | 0.0141 |

method was once again needed this time. However, when the objective was accurate width predictions for new process settings, the 3NN technique yielded the highest correlation coefficient, albeit a limited one. It can be observed that the 3NN method provides the best correlation out of all the kNN

simulations that were analysed. Again, from the industrial point of view, this provides quite an intuitive technique. The prediction is made based on averaging the width from the 3 most similar process settings. However, the lowest MAE rate for kNN methods is observed for $k = 1$. **This clearly shows that the best model in terms of one criterion is not necessarily the best model under another criterion.** As already observed for width modelling, linear regression models do not achieve the desired accuracy; this result fits well with the conclusion presented in “Experimental results and discussion” section, that channel width depends mainly on scanning speed and pulse intensity and that this dependency is clearly not linear. **The substantial difference between the training and testing error rates for the multilayer perceptron suggests that a larger data set could be useful to improve the generalisation capa-**

Table 8 Accuracy of different models of laser milling depth

| | 1NN | 2NN | 3NN | 4NN | 5NN | Linear regression | Decision tree | Multilayer perceptron |
|-------|-------|-------|-------|-------|-------|-------------------|---------------|-----------------------|
| R^2 | 0.870 | 0.870 | 0.819 | 0.799 | 0.807 | 0.818 (0.839) | 0.871 (0.955) | 0.887 (0.940) |
| MAE | 2.04 | 2.04 | 2.60 | 2.81 | 2.80 | 2.90 | 2.31 | 2.17 |

Table 9 Accuracy of different models of laser milling width

| | 1NN | 2NN | 3NN | 4NN | 5NN | Linear regression | Decision tree | Multilayer perceptron |
|-------|-------|-------|--------------|-------|-------|-------------------|---------------|-----------------------|
| R^2 | 0.325 | 0.325 | 0.393 | 0.364 | 0.348 | 0.367 (0.441) | 0.371 (0.638) | 0.317 (0.606) |
| MAE | 1.82 | 1.82 | 1.95 | 2.07 | 2.14 | 2.09 | 2.18 | 2.62 |

Table 10 Accuracy of different models of laser milling surface roughness

| | 1NN | 2NN | 3NN | 4NN | 5NN | Linear regression | Decision tree | Multilayer perceptron |
|-------|-------|-------|-------|-------|-------|----------------------|---------------|-----------------------|
| R^2 | 0.090 | 0.090 | 0.205 | 0.236 | 0.305 | 0.323 (0.417) | 0.076 (0.595) | 0.303 (0.481) |
| MAE | 0.043 | 0.043 | 0.035 | 0.034 | 0.033 | 0.030 | 0.038 | 0.038 |

Table 11 Accuracy of different models of laser milling surface roughness—part II

| | 6NN | 7NN | 8NN | 9NN | 10NN | 11NN | 12NN | 13NN | 14NN | 15NN |
|-------|-------|-------|-------|-------|-------|-------|-------|-------|-------|-------|
| R^2 | 0.242 | 0.231 | 0.263 | 0.264 | 0.240 | 0.152 | 0.116 | 0.100 | 0.096 | 0.090 |
| MAE | 0.034 | 0.033 | 0.032 | 0.033 | 0.034 | 0.036 | 0.037 | 0.037 | 0.037 | 0.038 |

Table 12 Accuracy of different models of laser milling MRR

| | 1NN | 2NN | 3NN | 4NN | 5NN | Linear regression | Decision tree | Multilayer perceptron |
|----------------|--------------|-------|-------|-------|-------|-------------------|---------------|-----------------------|
| R ² | 0.769 | 0.769 | 0.680 | 0.650 | 0.657 | 0.702 (0.741) | 0.689 (0.825) | 0.668 (0.828) |
| MAE | 0.006 | 0.006 | 0.007 | 0.007 | 0.008 | 0.007 | 0.007 | 0.008 |

bilities of the neural networks i.e. the ability to accurately predict width under new process settings.

In the case of surface roughness modeling, an interesting phenomenon was observed (Tables 10, 11). The correlation coefficient values appeared to grow at higher values of k , which led us to conduct an extended analysis of the values of k that exceeded 5, as shown in Table 11.

As expected, the value of the correlation coefficient deteriorates for $k > 5$. Obviously, it will converge to naïve results i.e. error rates attained when mean roughness value is returned as prediction. The main conclusion here is that the impact of process settings on surface roughness is quite sophisticated and possibly noisy, as averaging roughness from $k = 5$ most similar experiments yielded the best roughness prediction out of all kNN experiments. At the same time, the best overall correlation coefficient value and MAE rate was attained for cross-validation for linear regression (in bold in Table 10) and for training data for decision trees and was superior to kNN. As already observed for width and depth modelling, the linear regression models did not achieve the expected accuracy. At the same time, the nonlinear models, namely decision trees and multilayer perceptrons did not yield sufficient generalisation - i.e. high correlation in cross-validation -, in all probability due to the limited size of the data set. However, the nonlinear models and especially the decision trees were capable of modelling the dependencies in the training data with much higher accuracy than linear regression. This result fits in well with the conclusion in “Experimental results and discussion” section, which states that channel roughness depends mainly on scanning speed with a very noisy dependency, which in no case is ever linear.

In the case of MRR modelling, Table 12, multilayer perceptrons and decision trees yield the best and virtually identical results on the training data set. In this case, 1NN proves to be the best method out of kNN methods for k ranging from 1 to 5 and the best in terms of its generalisation capabilities i.e. the correlation coefficient for cross-validation runs. This is in line with previous findings for depth i.e. the closest input settings produce the most similar output parameter value: this time, the MRR rates. Linear regression models do not achieve the required accuracy; this result fits in well with the conclusion presented in “Experimental results and discussion” section, that MRR depends mainly on pulse intensity (more than 93 % in the ANOVA test) and that this dependency is not linear.

To sum up prediction accuracy evaluation, depth and MRR can be modelled with high accuracy. Lower, but still significant accuracy in comparison with the naïve baseline, was observed for surface roughness and width modelling. In the case of surface roughness, a higher value of k , meaning the averaging of roughness based on many similar experiments gave better results than using the roughness from the most similar experiment in terms of input settings. This observation points to noisy data, dependencies between inputs and outputs that are difficult to capture and even the need to collect other parameter values that contribute to the problem. In accordance with the bibliography (Benardos and Vosniakos 2003), it can be concluded that surface roughness depends on too many variables to assure a complete determination of the milling process, which means that all models will inevitably be less accurate than the other performance parameters under study. In no case did the linear regressions show high accuracy, which was expected, considering the non-linear dependencies between the input and the output parameters in all cases.

The selection of machine-learning parameters in the example of decision trees

One of the most accurate of the above-described techniques is the decision tree. The function of a decision tree is to predict the value of the parameter of interest. This process will be discussed in relation to the example of the depth parameter. Decision trees were used in this case in the following way. First, the domain of depth value was divided into 15 ranges. Next, the function of the decision tree was to predict the range of the depth value for the process parameters. A sample tree developed for the whole available data set is shown in Fig. 7 and has been discussed earlier in the paper.

However most machine-learning techniques are controlled with additional parameters, such as k for kNN technique or the number of neurons in a hidden layer for multilayer perceptrons. Hence, the question is whether the default parameter settings will yield the most accurate results. To answer this question, parameter tuning can be performed. This is frequently based on some heuristics or by testing different values in the domain of the parameter. To illustrate this process, the search for a C parameter that controls the decision tree construction is performed. Its default value, used to construct the decision trees is 0.25. The parameter is used

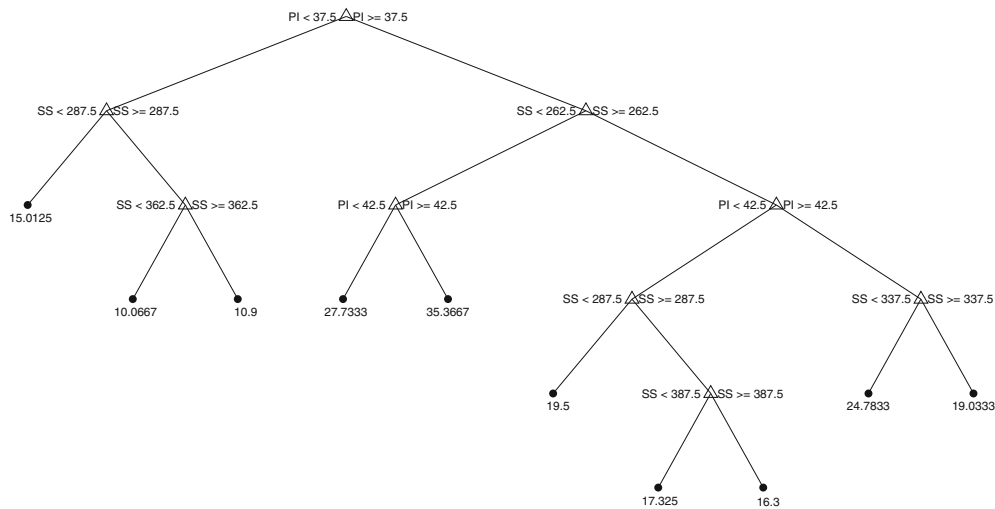


Fig. 7 Decision tree for the estimation of depth

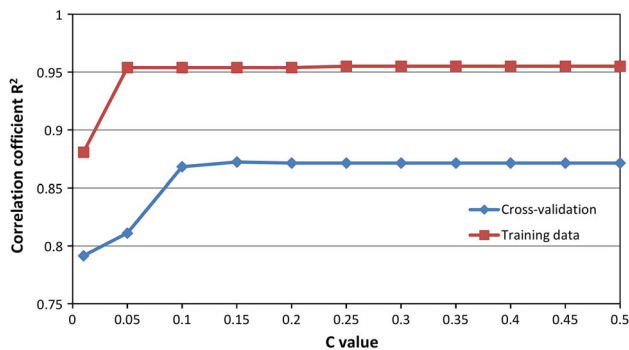


Fig. 8 The impact of the C parameter on the accuracy of the decision trees built for depth and tested on the training set and on the testing subsets. The cross-validation series shows the results attained on the testing subsets in cross-validation

for tree pruning and its smaller values incur more restrictive pruning. Hence, by varying the parameter, we may expect smaller or larger tree structures yielding predictions that differ from those generated by the tree constructed with the default settings.

Thus, the tree construction process was repeated for different C values in the domain $(0, 0.5]$. For each setting, the averaged correlation coefficient calculated on the testing subsets of a 10-fold cross-validation was calculated. Moreover, the correlation coefficient showing the similarity of the actual depth value and depth predicted by the decision tree was calculated on the entire training data sets. This was done for decision trees constructed with this entire training data set. The results of these experiments are summarized in Fig. 8.

It follows from this figure that constant quality may be observed, at C values higher than 0.25, for the decision trees constructed in the cross-validation process and with the training set. Should a C value below 0.1 be used, this will negatively affect the accuracy of the models. For all C values, the correlation reported for the data used in tree construction

(the training data) is higher than the correlation for the new process settings not used in the tree construction and present in individual testing folders of cross-validation. Finally, it can be observed that the best accuracy on the training set is observed for C values of 0.25 and above. However, the best generalization ability shown by the highest value of R^2 for cross-validation is observed for $C = 0.15$. This clearly illustrates the fact that an overly complex model will respond properly for the data used to construct it i.e. the training data, but will lose its capability to predict the parameter of interest, in this case depth, for new input data i.e. new process settings. On the other hand, the simulations show that a default value of $C = 0.25$ in the analysed case was close to optimal in terms of model accuracy observed in cross-validation. Taking into account the overall results of the experiments discussed above, a C value in the range $(0.15, 0.25)$ can be used to develop a decision tree model for depth. Such a model can be used in industrial applications to predict the depth value for new process settings and to show the impact of known process settings on depth value.

Parameter tuning can be performed in a similar way for other machine-learning methods and their parameters. This process can also be repeated for the remaining output features.

Industrial application

From the industrial point of view, it is not sufficient to demonstrate that the tested machine-learning techniques can develop accurate models. Certain figures of merit or, better still, certain plots are required, so that the workshop can take advantage of the information held by the model. The developed models consider three of the input parameters that can be easily changed in any real laser-milling centre: scanning speed, pulse intensity and pulse frequency. Therefore

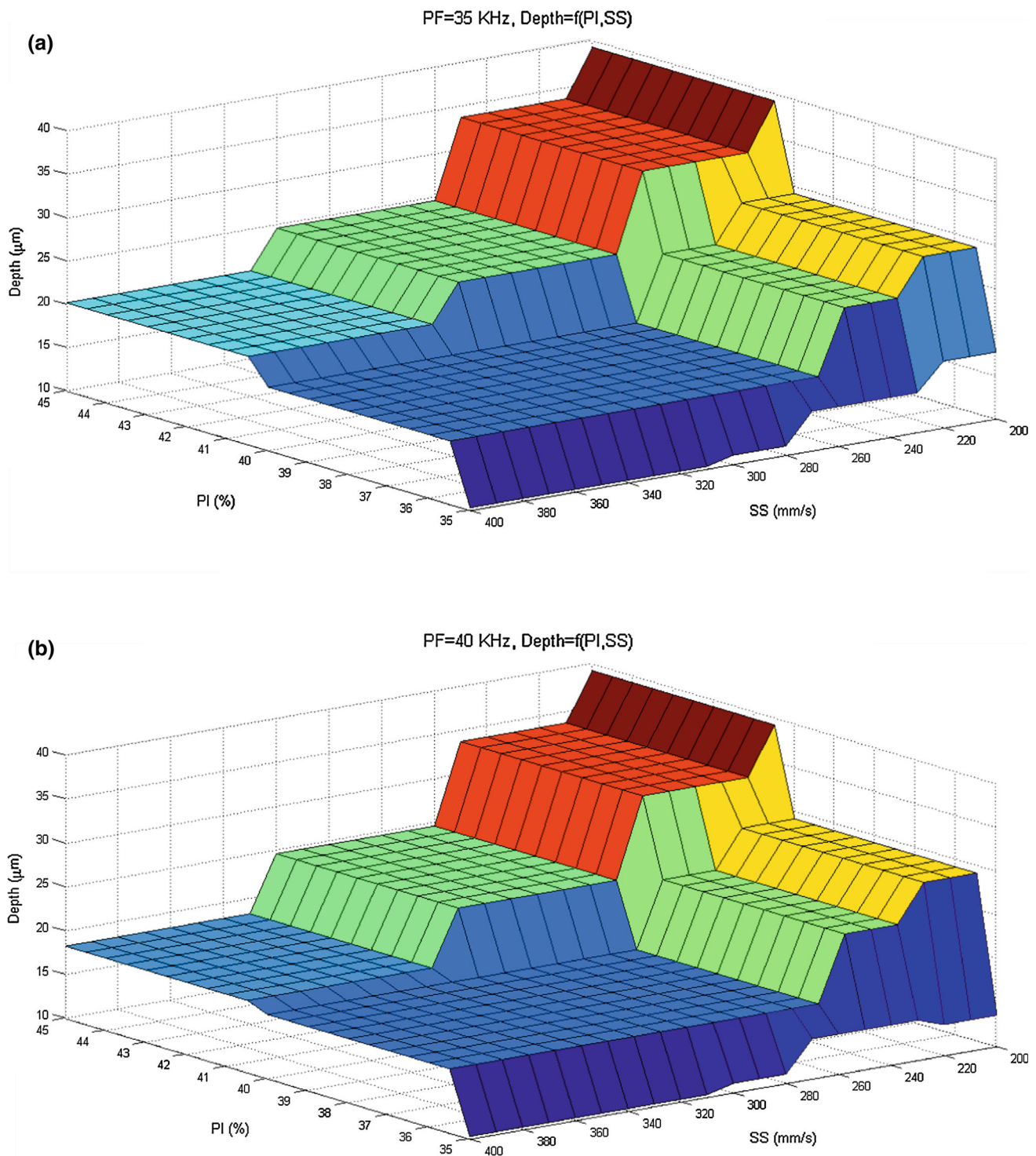


Fig. 9 Channel depth prediction with a Decision Tree model under different PI, PS and SS conditions: **a** PF = 35 KHz and **b** PF = 40 KHz

the modification of any of these parameters in a real situation can be done immediately. **In our case, the model should assist technicians in preparing the Computer Aided Manufacturing (CAM) program.** This program fixes laser trajectories and milling conditions to machine the channels. Therefore,

a plot that provides information on how the laser-milling conditions (SS, PI and PS) affect the geometry and surface roughness of a channel as well as milling productivity would be very useful. To do so, the following procedure was followed:

- First of all, four models using Decision Trees to predict the four outputs were developed. The models were trained using all the real data collected during experiments.
- Then, the four models were programmed to predict their respective outputs for a grid of laser-milling conditions that covers the whole experimental range of the three process variables (SS, PI and PS). 20 steps were fixed for each variable range, giving a total of 9261 laser-milling conditions ($21 \times 21 \times 21$) to be predicted.
- Because only 3 variables can be shown on a 3D plot, different 3D plots were drawn with the predicted variable on the Z-Axis and using the X and the Y-Axis to show the two process variables with a higher influence in the output variable behavior for a fixed value of the third process variable.

One example will easily show the beneficial results of applying this methodology. Figure 9a, b show the predicted depth of a channel as a function of PI and SS for two fixed values of PF (the two limits of the variation range of this variable: 35 and 40 KHz). The first conclusion is that the influence of PF is almost negligible, because both plots are almost the same. This result was expected from the ANOVA analysis that gave a 2.4 % contribution to depth. Three main flat surfaces can be defined in the 3D Plot that would allow the workshop technicians to identify the best laser-milling conditions depending in the desired depth. For example, if a depth of 25 μm is desired, SS should be fixed in the range of (280–320) mm/s and PI in the range of (41–45) %. For higher depths, SS should be smaller than 280 mm/s and PI kept in the range of (41–45) %. At smaller depths (of around 20 μm), SS should be higher than the 300 mm/s range and PI smaller than 39 %.

Conclusions

Micro-laser milling is a machining process suitable for fabricating micro-moulds. However, it requires highly tuned process parameters settings. In this study, surface quality, dimensional features and the productivity of micro-channels have been studied in a micro-laser milling process. Although the results obtained for the micro-channels present variations, they do suggest that laser machining is capable of producing micro-geometries. Several specific conclusions should be pointed out:

1. Low scanning speeds and high pulse intensities increase the depth and decrease the width of the micro-channels.
2. The surface quality of the channels improves with a rise in scanning speed, which in turn decreases surface roughness.
3. Laser micromachining productivity increases with high pulse intensities and low scanning speeds.

4. ANOVA results show that pulse frequency is not statistically significant for the responses under study.
5. Machine-learning techniques are suitable techniques with which to model laser-milling manufacture of micro shapes. Higher accuracy is observed for depth and material removal rate modelling, than for surface roughness and width modelling. Neural networks were a bit better at modelling depth dimensions and decision trees were better at modelling MRR; both techniques were similar for width and surface roughness. In general, these two techniques showed better accuracy than the other two models: k-nearest neighbours and linear regression. The use of decision trees is therefore feasible, if information on the relation between input parameters is sought, while neural networks are better where the main industrial requirement is the dimensional accuracy of the workpiece.
6. The Nearest Neighbour models with higher k values show greater accuracy for roughness prediction, allowing us conclude that the noisiness of this output is higher or that it depends on more parameters than the other variables, as suggested in the previous literature. Datasets of a larger size (52 instances for 3 input parameters) are necessary to increase the accuracy of the most accurate models: Decision Trees and MLPs.

Future work will consider other AI techniques, such as ensembles of classifiers or regressors. These ensembles are built by combining different basic classifiers that could improve final model accuracy. Non-linear models will also be tested, such as non-linear regressors, to ensure that any interaction effect is taken into account and evaluated. This experimental methodology, in which the best process parameter combination is selected, will also be applied to other types of materials, such as transparent polymers typically used for disposable lab-on-chip devices and ceramics used for various industrial applications in aeronautics, automobile manufacturing, electronics, medicine, and semiconductors. Moreover, other process parameters will be considered as input attributes to be added to the model, in order to make it more reliable and precise.

Acknowledgments This study was partially supported through grants from the European Commission project IREBID (FP7-PEOPLE-2009-IRSES-247476) and the Spanish Science and Innovation Minister project TECNIPLAD (DPI2009-09852).

References

- Bartolo, P., Vasco, J., Silva, B., & Galo, C. (2006). Laser micromachining for mould manufacturing: I. The influence of operating parameters. *Assembly Automation*, 26(3), 227–234.
- Bordatchev, E. V., & Nikumb, S. K. (2003). An experimental study and statistical analysis of the effect of laser pulse energy on the

- geometric quality during laser precision machining. *Machine Science Technology*, 7(1), 83–104.
- Benardos, P. G., & Vosniakos, G. C. (2003). Predicting surface roughness in machining: A review. *International Journal of Machine Tools and Manufacture*, 43(8), 833–844.
- Brousseau, E., & Eldukhri, E. (2011). Recent advances on key technologies for innovative manufacturing. *Journal of Intelligent Manufacturing*, 22(5), 675–691.
- Bustillo, A., & Correa, M. (2012). Using artificial intelligence to predict surface roughness in deep drilling of steel components. *Journal of Intelligent Manufacturing*, 23(5), 1893–1902.
- Bustillo, A., Díez-Pastor, J. F., Quintana, G., & García-Osorio, C. (2011a). Avoiding neural network fine tuning by using ensemble learning: application to ball-end milling operations. *The International Journal of Advanced Manufacturing Technology*, 57(5), 521–532.
- Bustillo, A., Ukar, E., Rodriguez, J. J., & Lamikiz, A. (2011b). Modelling of process parameters in laser polishing of steel components using ensembles of regression trees. *International Journal of Computer Integrated Manufacturing*, 24(8), 735–747.
- Campanelli, S. L., Ludovico, A. D., Bonserio, C., Cavalluzzi, P., & Cinquepalmi, M. (2007). Experimental analysis of the laser milling process parameters. *Journal of Materials Processing Technology*, 191(1–3), 220–223.
- Cicală, E., Soveja, A., Sallamand, P., Grevey, D., & Jouvard, J. M. (2008). The application of the random balance method in laser machining of metals. *Journal of Materials Processing Technology*, 196(1–3), 393–401.
- Chandrasekaran, M., Muralidhar, M., Krishna, C., & Dixit, U. (2010). Application of soft computing techniques in machining performance prediction and optimization: A literature review. *International Journal of Advanced Manufacturing Technology*, 46(5), 445–464.
- Ciurana, J., Arias, G., & Ozel, T. (2009). Neural network modeling and particle swarm optimization (PSO) of process parameters in pulsed laser micromachining of hardened AISI H13 steel. *Materials and Manufacturing Processes*, 24(3), 358–368.
- Correa, M., Bielza, C., & Pamies-Teixeira, J. (2009). Comparison of Bayesian networks and artificial neural networks for quality detection in a machining process. *Expert Systems with Applications*, 36, 7270–7279.
- Desai, C. K., & Shaikh, A. (2012). Prediction of depth of cut for single-pass laser micro-milling process using semi-analytical, ANN and GP approaches. *International Journal of Advanced Manufacturing Technology*, 60(9–12), 865–882.
- Dhara, S. K., Kuar, A. S., & Mitra, S. (2008). An artificial neural network approach on parametric optimization of laser micro-machining of die-steel. *International Journal of Advanced Manufacturing Technology*, 39(1–2), 39–46.
- Díez-Pastor, J. F., Bustillo, A., Quintana, G., & García-Osorio, C. (2012). Boosting projections to improve surface roughness prediction in high-torque milling operations. *Soft Computing*, 16(8), 1427–1437.
- Grzenda, M., Bustillo, A., Quintana, G., & Ciurana, J. (2012a). Improvement of surface roughness models for face milling operations through dimensionality reduction. *Integrated Computer-Aided Engineering*, 19(2), 179–197.
- Grzenda, M., Bustillo, A., & Zawistowski, P. (2012b). A soft computing system using intelligent imputation strategies for roughness prediction in deep drilling. *Journal of Intelligent Manufacturing*, 23(5), 1733–1743.
- Karazi, S. M., Issa, A., & Brabazon, D. (2009). Comparison of ANN and DoE for the prediction of laser-machined micro-channel dimensions. *Optics and Lasers in Engineering*, 47, 956–964.
- Kaldos, A., Pieper, H. J., Wolf, E., & Krause, M. (2004). Laser machining in die making—a modern rapid tooling process. *Journal of Materials Processing Technology*, 155–156, 1815–1820.
- Kumar, A., & Gupta, M. C. (2010). Laser machining of micro-notches for fatigue life. *Optics and Lasers in Engineering*, 48(6), 690–697.
- Mahdavinejad, R. A., Khani, N., & Fakhraabadi, M. M. S. (2012). Optimization of milling parameters using artificial neural network and artificial immune system. *Journal of Mechanical Science and Technology*, 26(12), 4097–4104.
- Pham, D. T., Dimov, S. S., & Petkov, P. V. (2007). Laser milling of ceramic components. *International Journal of Machine Tools Manufacturing*, 47(3–4), 618–626.
- Quintana, G., Bustillo, A., & Ciurana, J. (2012). Prediction, monitoring and control of surface roughness in high-torque milling machine operations. *International Journal of Computer Integrated Manufacturing*, 25(12), 1129–1138.
- Quintana, G., Garcia-Romeu, M. L., & Ciurana, J. (2011). Surface roughness monitoring application based on artificial neural networks for ball-end milling operations. *Journal of Intelligent Manufacturing*, 22, 607–617.
- Rizvi, N. H., & Apte, P. (2002). Developments in laser micro-machining techniques. *Journal of Materials Processing Technology*, 127(2), 206–210.
- Samant, A. N., & Dahotre, N. B. (2010). Three-dimensional laser machining of structural ceramics. *Journal of Manufacturing Processes*, 12(1), 1–7.
- Semaltianos, N. G., Perrie, W., Cheng, J., French, P., Sharp, M., Dear-den, G., et al. (2010). Picosecond laser ablation of nickel-based superalloy C263. *Applied Physics A: Materials Science and Processing*, 98(2), 345–355.
- Yousef, B. F., Knopf, G. K., Bordatchev, E. V., & Nikumb, S. K. (2003). Neural network modeling and analysis of the material removal process during laser machining. *International Journal of Advanced Manufacturing Technology*, 22(1–2), 41–53.